Accounts

Chalcogenide Cluster Complexes of Chromium, Molybdenum, Tungsten, and Rhenium

Taro Saito* **and Hideo Imoto**

Department of Chemistry, School of Science, The University of Tokyo, Hongo, Tokyo 113

(Received April 22, 1996)

Trinuclear, tetranuclear, hexanuclear, and dodecanuclear chalcogenide cluster complexes of chromium, molybdenum, tungsten, and rhenium have been synthesized and their molecular and electronic structures have been characterized. The structure-cluster valence electron relationships are analyzed and a new isoelectronic analogy is proposed.

Cluster chemistry of the early transition metals with π-donor ligands (halide, oxide, chalcogenide, alkoxide) has progressed rapidly in recent years.[1] Among such ligands, chalcogens (S, Se, Te) are the most versatile anionic ligands. They show various types of ligation (terminal, μ_2-, μ_3-, or μ_4-bridging modes) to the metals, giving a variety of cluster complexes and solid state compounds.[2—18]

The rapid growth of this field is related to the biological cluster complexes,[19,20] and to the superconducting materials.[14] However, the chemistry of metal cluster compounds with π-donor ligands per se is very important as the basic chemistry of synthesis, cluster bonding and structure, reactions, and solid state properties. It is necessary to establish the rational construction of basic cluster frameworks to study the cooperative phenomena induced by the cluster structures.

Our study in this area was initiated from our interest in the structural problems in the superconducting Chevrel phases. We aimed at the preparation of the molecular complexes with similar octahedral cluster units to those in the solid state Chevrel phases.[21] We had been interested in the chemistry of octahedral halide cluster complexes of molybdenum[22] and tungsten[23] prior to this work on the chalcogenide cluster complexes. Since then, the general purpose of our research has been the development of rational syntheses of the cluster complexes related to the solid state cluster compounds.[24]

Rational Syntheses and Structures of New Cluster Complexes

Strategies in cluster synthesis have been applied to the preparation of chalcogenide cluster complexes with considerable success.[2] The basic patterns of the synthetic reactions are excision (or extrusion), cluster condensation, and self-assembly reactions. Excision is the bridge bond cleavage to cut out molecular clusters from solid state cluster compounds with the cluster units linked one-, two-, or three-dimensionally by bridging halide ligands.[25,26] Either neutral ligands or inorganic halides are used for the bond cleavage. Cluster condensation gives higher clusters by the removal of a part of anionic or neutral ligands from smaller cluster complexes which are to be condensed and thus has higher selectivity than that of self-assembly reactions.[24] Self-assembly reactions have proved most fruitful in giving various kinds of new cluster compounds, although most of them have resulted from either thermodynamic or kinetic control to form certain cluster frameworks preferentially and it is difficult to predict the products.[11] We have used these methods to prepare new kinds of chromium, molybdenum, tungsten, and rhenium cluster complexes. (Table 1)

Trinuclear Molybdenum Cluster Complexes. The reaction of $Mo_3(\mu_3\text{-}S)(\mu_2\text{-}S_2)_3Cl_2Cl_{4/2}$[27,28] with triethylphosphine in tetrahydrofuran, followed by recrystallization from methanol, afforded two kinds of cluster complexes $[Mo_3(\mu_3\text{-}S)(\mu_2\text{-}S)_3Cl_4(PEt_3)_3(MeOH)_2]$ **1** and $[Mo_3(\mu_3\text{-}S)(\mu_2\text{-}S)_3Cl_4(PEt_3)_4(MeOH)]$.[29] The structure of **1** is shown in Fig. 1. The cluster core is the isosceles triangle of Mo_3 capped by a sulfur, and each Mo–Mo edge is bridged by a sulfur atom. Four terminal chlorine ligands are bound to molybdenum atoms as well as three triethylphosphine and two methanol ligands. The essential reaction in the preparation is abstraction of one of the two sulfur atoms from the S_2 bridges of the solid state compound by triethylphosphine, with cleavage of the chlorine bridges between the cluster units. This type of excision reaction was reported for the first time by a Russian group for the preparation of $[Mo_3(\mu_3\text{-}S)(\mu_2\text{-}S)_3Cl_4(PPh_3)_2]$ in acetonitrile.[30] The major difference in their compounds is the number of neutral ligands. Similar reactions have been employed later for the preparation of

Table 1. Preparative Method and MCE and of the Chalcogenide Cluster Compexes

Compounds	Starting compounds/solvent	MCE[a)]	Ref.
$[Mo_3S_4Cl_4(PEt_3)_3(MeOH)_2]$	$Mo_3S_7Cl_4$, PEt_3, MeOH/THF	6	29
$[Mo_3S_4Cl_4(PEt_3)_4(MeOH)]$	$Mo_3S_7Cl_4$, PEt_3, MeOH/THF	6	29
$[Mo_3S_4Cl_4(py)_5]$	$Mo_3S_7Cl_4$, PPh_3/py	6	33
$[W_3S_4Br_3(OAc)(CH_3CN)(PEt_3)_3]$	$W_3S_7Br_4$, PEt_3, MeOH/THF	6	37
$[Mo_3S_4Cl_3(dppe)_2(PEt_3)_3]$	$Mo_3S_7Cl_4$, PEt_3, dppe, Mg/THF, hexane	7	38
$[Mo_3S_5(PMe_3)_6]$	$(NH_4)_2Mo_3S_{13}$, PMe_3/THF	8	34
$[Re_3S_4Cl_4(PEt_3)_3]$	$Re_3S_7Cl_7$, PEt_3/THF, acetone	9	36
$[Mo_4S_6(SH)_2(PMe_3)_6]$	$(NH_4)_2Mo_3S_{13}$, PMe_3/$BuNH_2$	10	49
$[Mo_4S_6Cl_2(PMe_3)_6]$	$[Mo_4S_6(SH)_2(PMe_3)_6]$, $SnCl_2$/THF	10	49
$[Mo_4S_6Br_2(PMe_3)_6]$	$[Mo_4S_6(SH)_2(PMe_3)_6]$, $SnBr_2$/THF	10	49
$[Mo_4S_6I_2(PMe_3)_6]$	$[Mo_4S_6(SH)_2(PMe_3)_6]$, SnI_2/THF	10	49
$[Mo_4S_6(dtc)_2(PMe_3)_4]$	$[Mo_4S_6Br_2(PMe_3)_6]$, Na(dtc)/THF	10	49
$[Mo_6S_{10}(SH)_2(PEt_3)_6]$	$(NH_4)_2Mo_3S_{13}$, PEt_3/THF	14	46
$[Mo_6S_8Cl_2(PEt_3)_6]$	$Mo_3S_7Cl_4$, PEt_3, Mg/THF	14	50
$[Mo_6Se_8Cl_2(PEt_3)_6]$	$Mo_3Se_7Cl_4$, PEt_3, Mg/THF	14	50
$[W_6S_8Cl_2(PEt_3)_6]$	$W_3S_7Cl_4$, PEt_3, Mg/THF	14	37
$[Cr_6S_8(PMe_3)_6]$	$CrCl_2$, Na_xSH, PMe_3/MeOH	20	60
$[Cr_6S_8(PEt_3)_6]$	$CrCl_2$, NaS_xH, PEt_3/MeOH	20	60
$[Cr_6Se_8(PMe_3)_6]$	$CrCl_2$, Na_2Se_x, PMe_3/MeOH	20	60
$[Cr_6Se_8(PEt_3)_6]$	$CrCl_2$, Na_2Se_x, PEt_3/MeOH	20	60
$[Cr_6Se_8(PMe_2Ph)_6]$	$CrCl_2$, Na_2Se_x, PMe_2Ph/MeOH	20	60
$[Mo_6S_8(PMe_3)_6]$	$Mo_3S_7Cl_4$, PMe_3, Mg/THF	20	52
$[Mo_6S_8(PEt_3)_6]$	$Mo_3S_7Cl_4$, PEt_3, Mg/THF	20	51
$[Mo_6S_8(PMe_2Ph)_6]$	$Mo_3S_7Cl_4$, PMe_2Ph, Mg/THF	20	52
$[Mo_6Se_8(PEt_3)_6]$	$Mo_3Se_7Cl_4$, PEt_3, Mg/THF	20	51
$[W_6S_8(PEt_3)_6]$	$W_3S_7Cl_4$, PEt_3, Mg/THF	20	32
$[PPN][Mo_6S_8(PEt_3)_6]$	$[Mo_6S_8(PEt_3)_6]$, NaHg, PPNCl/THF	21	51
$[PPN][Mo_6Se_8(PEt_3)_6]$	$[Mo_6Se_8(PEt_3)_6]$, NaHg, PPNCl/THF	21	51
$[Mo_3Ni_2S_4Cl_4(PEt_3)_5]$	$[Mo_3S_4Cl_4(PEt_3)_3(MeOH)_2]$, $[Ni(cod)_2]$/THF	26	70
$[Mo_3Pt_2S_4Cl_4(PEt_3)_6]$	$[Mo_3S_4Cl_4(PEt_3)_3(MeOH)_2]$, $[Pt(cod)_2]$/THF	26	71
$[Cr_{12}S_{16}(PEt_3)_{10}]$	$[Cr_6S_8(PEt_3)_6]$, S_8/toluene	40	67
$[Mo_{12}S_{16}(PEt_3)_{10}]$	$[Mo_6S_8(PEt_3)_6]$, S_8/toluene	40	69

a)Metal cluster electron.

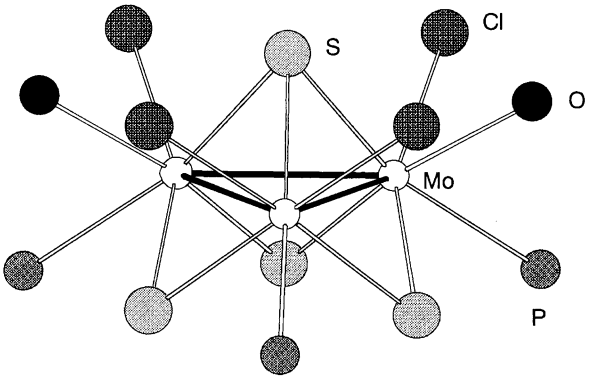

Fig. 1. Structure of $[Mo_3S_4Cl_4(PEt_3)_3(MeOH)_2]$ **1**.

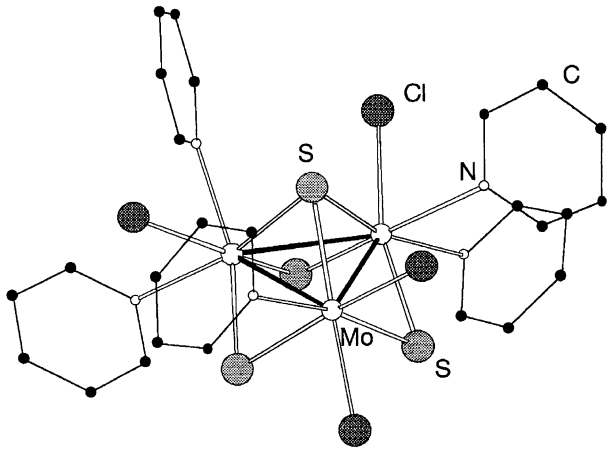

Fig. 2. Structure of $[Mo_3S_4Cl_4(py)_5]$ **2**.

other Mo_3S_4 cluster complexes and tungsten analogues.[31,32] When triphenylphosphine was reacted with $Mo_3(\mu_3\text{-}S)(\mu_2\text{-}S_2)_3Cl_2Cl_{4/2}$ in pyridine, a pyridine derivative $[Mo_3(\mu_3\text{-}S)(\mu_2\text{-}S)_3Cl_4(py)_5]$ **2** was obtained.[33] (Fig. 2) Triphenylphosphine abstracts one of the sulfur atoms in the μ_2-S_2 ligands, but does not coordinate to the Mo_3 core in the presence of a large amount of pyridine.

Treatment of $(NH_4)_2[Mo_3(\mu_3\text{-}S)(\mu_2\text{-}S_2)_3(S_2)_3]$ with trimethylphosphine in THF gave $[Mo_3(\mu_3\text{-}S)_2(\mu_2\text{-}S)_3(PMe_3)_6]$ **3** in 25% yield.[34] The oxidation state of molybdenum is reduced from +4 to +3.33 in the reaction. This reaction is an example of a new reaction in which removal of extra sulfur atoms in the S_2 ligands leads to a sulfur bi-capped cluster in contrast with the reactions of $Mo_3(\mu_3\text{-}S)(\mu_2\text{-}S_2)_3Cl_2Cl_{4/2}$ with trialkylphosphines to form Mo_3S_4 type clusters.[29] The structure is shown in Fig. 3. The molecule of **3** has an

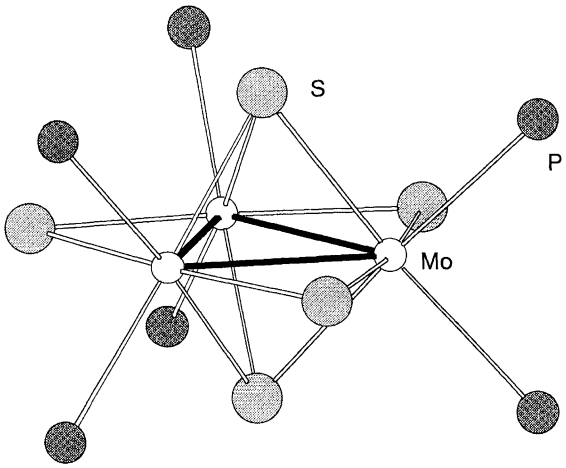

Fig. 3. Structure of $[Mo_3S_5(PEt_3)_6]$ **3**.

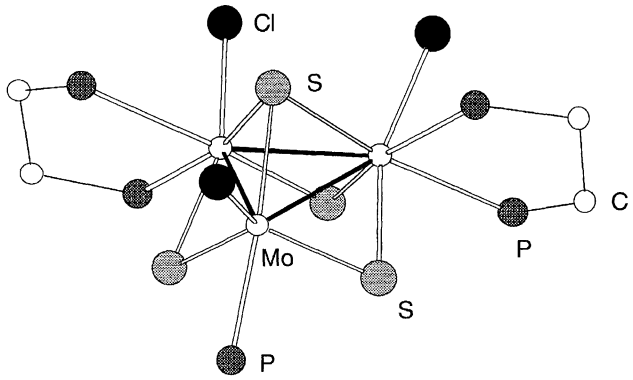

Fig. 4. Structure of $[Mo_3S_4Cl_3(dppe)_2(PEt_3)]$ **4**.

equilateral triangle of molybdenum atoms capped by two sulfur atoms and bridged by three sulfur atoms. There are six trimethylphosphines at the terminal positions of the Mo_3 triangle. The Mo–Mo distance is 2.71 Å, which is shorter than those in compounds of the Mo_3S_4 type (2.73—2.83 Å).

Another remarkable example of the desulfurization reaction of $[Re_3(\mu_3\text{-}S)(\mu_2\text{-}S_2)_3Cl_6]Cl$[35] by triethylphosphine has been found to give $[Re_3(\mu_3\text{-}S)_2(\mu_2\text{-}S)_2(\mu_2\text{-}Cl)Cl_3(PEt_3)_3]$.[36] In this case, one of the bridging positions is occupied by a chlorine atom and three chlorine and three triethylphosphine ligands are arranged in a chiral fashion.

The excision reaction of $W_3(\mu_3\text{-}S)(\mu_2\text{-}S_2)_3Br_2Br_{4/2}$ with triethylphosphine in THF, followed by treatment with acetic acid and recrystallization from acetonitrile, gave $[W_3(\mu_3\text{-}S)(\mu_2\text{-}S)_3Br_3(\mu_2\text{-}OAc)(PEt_3)_3(MeCN)]$ in 52% yield.[37] The cluster core is a $W_3(\mu_3\text{-}S)(\mu_2\text{-}S)_3$ type and each tungsten atom is coordinated by a bromine and a triethylphosphine ligand. One of the W–W edges is bridged by a bidentate acetate anion and one of the three tungsten atoms is coordinated by an acetonitrile. This reaction shows that ligand substitution of a stable cluster framework is a very useful method for the preparation of new cluster complexes.

Redox reaction is also a useful method for preparing new kinds of cluster complexes; usually the cluster cores are preserved with some distortions of the cluster geometry. The reduction of the Mo_3S_4 core is such a case. When the reaction product of $Mo_3(\mu_3\text{-}S)(\mu_2\text{-}S_2)_3Cl_2Cl_{4/2}$ with triethylphosphine was reduced with magnesium at −20 °C followed by addition of dppe (1,2-bisdiphenylphosphinoethane), a crystalline seven-electron cluster $[Mo_3(\mu_3\text{-}S)(\mu_2\text{-}S)_3Cl_3(dppe)_2(PEt_3)]$ **4** was isolated; its molecular structure is shown in Fig. 4.[38] The seven-electron cluster complex before the addition of dppe is considered to be a precursor to the 14-electron raft complex **7** (see below). Electrochemistry of some of the Mo_3S_4 type cluster complexes had shown the seven-electron and eight-electron stages[39—42] and two seven-electron clusters had been reported without X-ray study.[43,44] Very recently another seven-electron Mo_3S_4 cluster $[(Cp^*Mo)_3(\mu_3\text{-}S)(\mu_2\text{-}S)_3]$ has been prepared and structurally characterized.[45]

Tetranuclear Cluster Complexes. A novel tetranuclear cluster complex $[Mo_4(\mu_3\text{-}S)_2(\mu\text{-}S)_4(SH)_2(PMe_3)_6]$ **5** formed in the reaction of $(NH_4)_2[Mo_3(\mu_3\text{-}S)(\mu_2\text{-}S_2)_3(S_2)_3]$ with trimethylphosphine in butylamine.[46] The mean oxidation state of molybdenum is reduced from +4 to +3.5 in the formation of the tetranuclear cluster. There are a few possible pathways for the rearrangement of a trinuclear cluster into a tetranuclear cluster complex: 1) degradation of the trinuclear cluster to mononuclear species, which in turn assemble to a tetranuclear one; 2) formation of a dinuclear species which dimerizes; or 3) formation of a mononuclear species which adds to the trinuclear cluster. The fact that the yield of the reaction is fairly high (ca. 40% based on Mo) implies that the tetranuclear cluster is rather a stable one. In this regard, the recent report by Hidai et al. on the preparation of the analogous tungsten cluster complex $[W_4(\mu_3\text{-}S)_2(\mu_2\text{-}S)_4(SH)_2(PMe_2Ph)_6]$ from $[W(N_2)_2(PMe_2Ph)_4]$ with $(Me_3Si)_2S$ in the presence of methanol is suggestive of the ease of the formation of these tetranuclear cluster cores.[47] Shibahara also reported the conversion of $[Mo_3O_2S_2(H_2O)_9]^{4+}$ into $[Mo_4(\mu_3\text{-}S)_2(\mu_2\text{-}O)_4(H_2O)_{10}]^{4+}$.[48] The oxidation state of molybdenum is +4 and does not change in the transformation.

The cluster core of **5** (Fig. 5) is composed of four molybdenum atoms arranged in a rhombus geometry. Each of the fused Mo_3 triangles is capped by a sulfur atom and bridged by two sulfur atoms. In another view, the whole structure is composed of fusion of two incomplete cubanes. Each wingtip (if we regard the Mo_4 as a butterfly) molybdenum atom is bound to an SH group and a trimethylphospine ligand. The hinge molybdenum atoms are coordinated by two trimethylphosphine ligands. The SH groups have a stretching frequency in the infrared spectrum at 2516 cm^{-1}.

The terminal SH groups of **5** have been changed into halides by the reaction with stannous halides.[49] The reaction of the bromide with sodium diethyldithiocarbamate (Nadtc) gave a cluster complex $[Mo_4S_6(dtc)_2(PMe_3)_4]$ **6** (Fig. 6) with four trimethylphosphine ligands instead of six. The average oxidation state of the molybdenum atoms is +3.50 and the cluster complexes are mixed valence complexes of two Mo(III) and two Mo(IV). They have ten cluster valence electrons to form five Mo–Mo single bonds ranging from 2.818 to 2.845 Å.

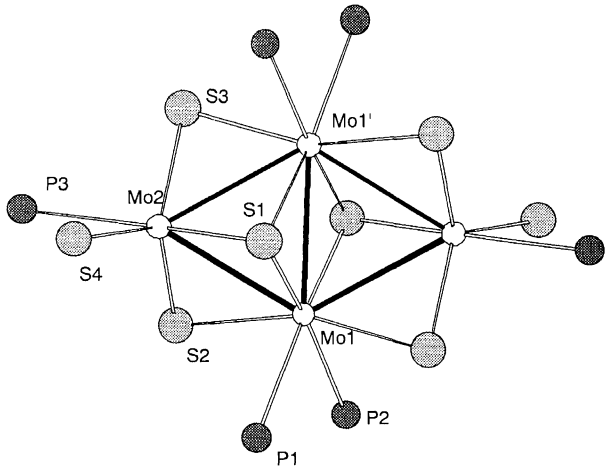

Fig. 5. Structure of $[Mo_4S_6(SH)_2(PMe_3)_6]$ **5**.

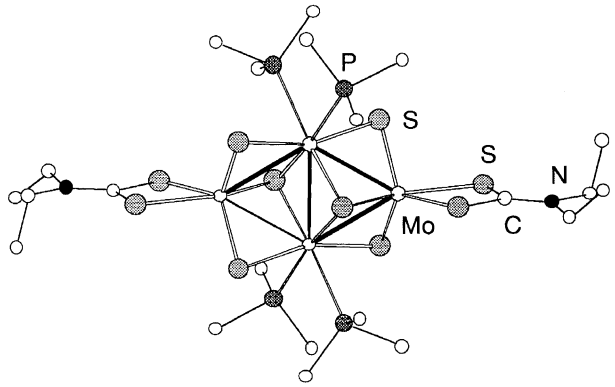

Fig. 6. Structure of $[Mo_4S_6(dtc)_2(PMe_3)_4]$ **6**.

Raft-Type Hexanuclear Cluster Complexes of Molybdenum and Tungsten. A raft of an edge-fused array of four triangles forms by combining two triangles in a plane (Scheme 1). The condensation of two triangular cluster complexes by abstraction of terminal ligands to form such structures can also be a general method to prepare hexanuclear or larger raft-type clusters. We have found that reduction of $[M_3E_4Cl_4(PEt_3)_n(thf)_{5-n}]$ (M = Mo, E = S, Se; M = W, E = S) with magnesium metal can be controlled. Namely only one terminal chlorine atom is removed to form metastable clusters $[M_3E_4Cl_3(PEt_3)_n(thf)_{6-n}]$ at lower temperatures. The removals of weakly ligating solvent (THF) by washing the intermediate complex with hexane forms coupled cluster complexes $[M_6E_8Cl_6]$ (M = Mo, E = S, Se;[50] M = W, E = S[37]).

The cluster framework of $[Mo_6(\mu_3\text{-}S)_4(\mu_2\text{-}S)_4(\mu_2\text{-}Cl)_2Cl_4(PEt_3)_6]$ **7** (Fig. 7) consists of six molybdenum atoms placed on a plane. Two incomplete-cubane-type Mo_3S_4 cluster units are bound by a Mo–Mo bond, two μ_3-S, and two

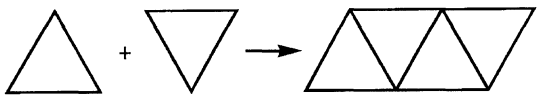

Scheme 1. Formation of a hexanuclear raft cluster from two triangular clusters.

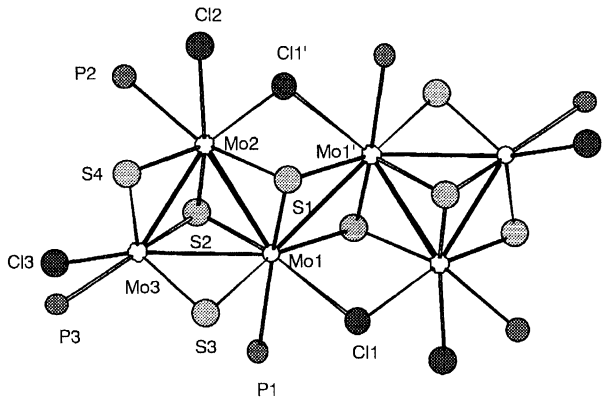

Fig. 7. Structure of $[Mo_6S_8Cl_6(PEt_3)_6]$ **7**.

μ_2-Cl. One triethylphosphine coordinates to each molybdenum atom, and a terminal chloro ligand coordinates to each of four molybdenum atoms. The selenium analogue has a very similar structure with longer Mo–Mo distances. The structure of $[W_6(\mu_3\text{-}S)_4(\mu_2\text{-}S)_4(\mu_2\text{-}Cl)_2Cl_4(PEt_3)_6]$ **8** (Fig. 8) is also similar to that of **7** and the W–W distances (2.748—2.997 Å) are longer than those of the Mo–Mo (2.693—2.993 Å) in **7**.

Treatment of$(NH_4)_2[Mo_3(\mu_3\text{-}S)(\mu_2\text{-}S_2)_3(S_2)_3]$ with triethylphosphine in THF formed another hexanuclear raft-type cluster complex $[Mo_6(\mu_3\text{-}S)_4(\mu_2\text{-}S)_6(SH)_2(PEt_3)_6]$.[46] The oxidation states of molybdenum atoms and overall structure of this complex are similar to those of **7**, but the number of terminal ligands decreases owing to the change of two of the bridging ligands from monovalent chlorine to divalent sulfur anions.

Octahedral Molybdenum and Tungsten Cluster Complexes. An octahedron is composed of two triangles stacked in a staggered way along the C_3 axis and the resultant deltahedron has eight triangular faces. The condensation of two triangular cluster complexes by abstraction of terminal ligands should be a general synthetic route to obtain hexanuclear cluster complexes with octahedral metal atom arrangements (Scheme 2). As almost the first example of such reactions, we have prepared $[Mo_6(\mu_3\text{-}S)_8(PEt_3)_6]$ **9** by reducing $[Mo_3(\mu_3\text{-}S)(\mu_2\text{-}S)_3Cl_4(PEt_3)_4(MeOH)]$ with magnesium in THF.[21]

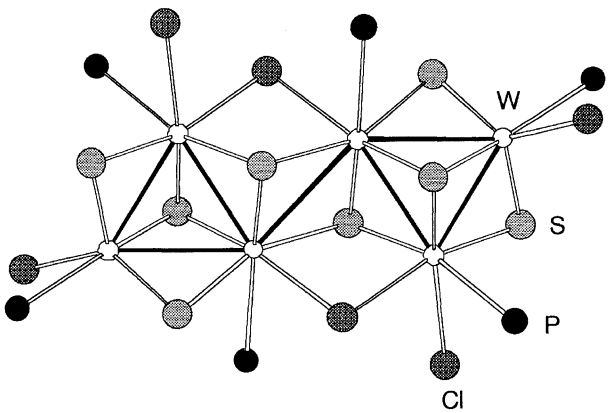

Fig. 8. Structure of $[W_6S_8Cl_6(PEt_3)_6]$ **8**.

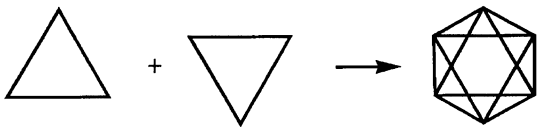

Scheme 2. Formation of an octahedral cluster from two triangular clusters.

Later the starting compounds have been changed to $[Mo_3(\mu_3\text{-}E)(\mu_2\text{-}E)_3Cl_4(PEt_3)_n(thf)_{5-n}]$ (E = S, Se) which are formed in the reaction of $Mo_3(\mu_3\text{-}E)(\mu_2\text{-}E_2)_3Cl_2Cl_{4/2}$ with triethylphosphine.[51] Other trialkylphosphines can be used,[52] and a similar tungsten derivative also has been prepared $[W_6(\mu_3\text{-}S)_8(PEt_3)_6]$ **10**.[32] Recently the octahedral molybdenum or tungsten cluster complexes $[M_6(\mu_3\text{-}E)_8L_6]$ (M=Mo, W; E=S, Se; L = py, pip, pyrr, *t*-Bupy) (py = pyridine, pip = piperidine, pyrr = pyrrole, *t*-Bupy = *t*-butylpyridine) have been prepared by the substitution of the face-capping chlorine atoms in $M_6(\mu_3\text{-}Cl)_8Cl_2Cl_{4/2}$ (M = Mo, W) into chalcogens.[53—56]

The cluster core of $[Mo_6(\mu_3\text{-}S)_8(PEt_3)_6]$ **9** (Fig. 9) is a regular octahedron of six molybdenum atoms with eight face-capping sulfur atoms and one triethylphosphine ligand coordinates to each of the molybdenum atoms. The tungsten derivative $[W_6(\mu_3\text{-}S)_8(PEt_3)_6]$ **10** (Fig. 10) has a very similar structure with slightly longer W–W distances (2.674—2.685 Å) than the Mo–Mo distances (2.662—2.664 Å) in **9**. These cluster complexes are mixed-valence complexes and the average oxidation state of the metals is +2.67 (4M(III)+2M(II)).

Octahedral Chromium Clusters. In case no solid state cluster compounds composed of suitable cluster units to be excised and no smaller cluster compounds to be condensed are known, we have to resort to self-assembly reactions in hopes of obtaining target compounds. After establishing the reductive dimerization reactions of trinuclear molybdenum or tungsten cluster complexes to prepare the Chevrel-type octahedral cluster, we wished to have chromium analogues. Unfortunately, no triangular chromium chalcogenide cluster complexes with terminal halogen ligands have been reported but it had long been known that cobalt and iron clusters with $[M_6(\mu_3\text{-}E)_8(PEt_3)_6]$ cores could be prepared by self-assembly

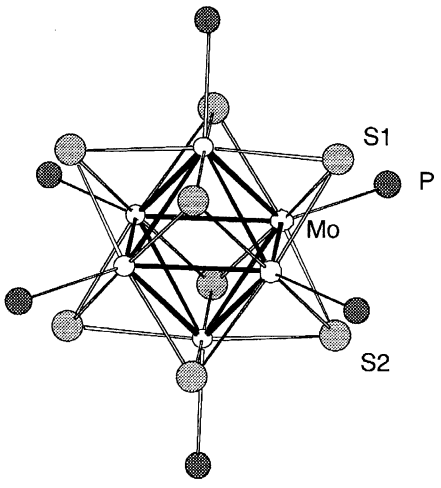

Fig. 9. Structure of $[Mo_6S_8(PEt_3)_6]$ **9**.

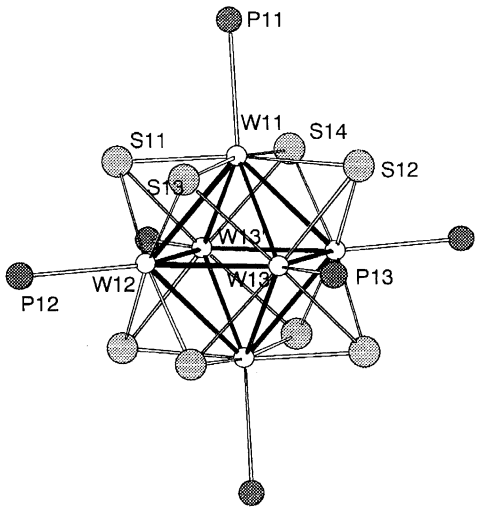

Fig. 10. Structure of $[W_6S_8(PEt_3)_6]$ **10**.

reactions starting from mononuclear complexes.[57,58] During our attempts to prepare elusive $[Cr_3(\mu_3\text{-}S)_2(\mu_2\text{-}S)_3(PMe_3)_6]$ by the reaction of $CrCl_2$ with NaSH in methanol, we found a very small amount of crystals of $[Cr_6(\mu_3\text{-}S)_8(PMe_3)_6]$.[59] The reaction has not been reproducible until we found that change of phosphine or chalcogen made the formation of the similar cluster complexes much easier. Although eventually we obtained the trimethylphosphine derivative again, the yields were very low. Several derivatives $[Cr_6(\mu_3\text{-}E)_8(PR_3)_6]$ (E=S, $R_3 = PMe_3$, PEt_3, PMe_2Ph; E = Se, $R_3 = PMe_3$, PEt_3) have been prepared and characterized structurally.[60] In the case of the sulfur derivatives, NaS_xH ($x = 1.33$) has been used while Na_2Se_x ($x = 1.33$) is better for the selenium clusters for a reason which has not become clear yet. The addition of the chalcogen source should be carried out at a very low temperature to prevent the formation of insoluble solid state chromium chalcogenides. Meanwhile, as the first example of Cr_6E_8 type cluster complexes, $[Cr_6(\mu_3\text{-}Te)_8(PEt_3)_6]$ has been published by Steigerwald.[61]

The structure of $[Cr_6(\mu_3\text{-}S)_8(PEt_3)_6]$ **11** (Fig. 11) comprises six chromium atoms arranged octahedrally with eight face-capping sulfur atoms and a triethylphosphine ligand coordinates to each chromium atom. The whole arrangement is very similar to the molybdenum or tungsten Chevrel-type cluster complexes **9** or **10**. The Cr–Cr distances are too long to invoke full single bonds. (see below)

A Dodecanuclear Chromium Cluster. In the Chevrel phase compounds, octahedral cluster units are linked by μ_4-S →Mo bondings.[62] Namely the capping sulfur atoms coordinate to the vacant molybdenum site in the adjacent cluster units, forming the three-dimensional network of octahedral Mo_6S_8 cluster units. This characteristic bridging mode brings about considerable intercluster Mo–Mo interaction which may be related to the superconductivity of the Chevrel phases.[63,64] One of the purposes of the preparation of the Chevrel-type molecular cluster complexes of the chromium group metals is to use them as the starting compounds to construct the solid state compounds resembling the

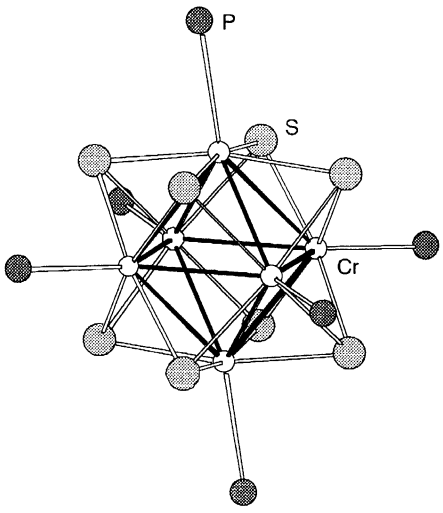

Fig. 11. Structure of $[Cr_6S_8(PEt_3)_6]$ **11**.

Chevrel phases.[53—56,61,65,66] The purpose has not been fulfilled yet, except for the case of the synthesis of $SnMo_6S_8$.[66] We have striven for a more modest goal of obtaining the dimers of the Chevrel-type cluster compounds in order to study the electronic and magnetic interactions between the octahedral cluster units through the μ_4-S $\rightarrow$M bondings. The strategy to attain the goal has been to remove one of the coordinated phosphines by reagents with higher affinity to phosphines than to the metals. After examining several reagents, we found that elemental sulfur is the best one. Thus the reaction of the chromium cluster $[Cr_6S_8(PEt_3)_6]$ **11**[60] with one equivalent of sulfur in toluene at the refluxing temperature gave a product which has been identified as $[Cr_{12}(\mu_4\text{-}S)_2(\mu_3\text{-}S)_{14}(PEt_3)_{10}]$ **12**.[67] The structure in Fig. 12 shows that the two octahedral cluster units are linked in the similar mode to that in the Chevrel phase molybdenum compounds. Only one example of dodecahedral cobalt complex has been reported.[68] A similar molybdenum analogue has been prepared.[69] The intercluster M–M bond distances in the three complexes are Co_{12} 2.64 Å, Cr_{12} 2.95 Å, and Mo_{12} 3.40 Å.

Mixed-Metal Cluster Complexes. The reaction of $[Mo_3(\mu_3\text{-}S)(\mu_2\text{-}S)_3Cl_4(PEt_3)_3(MeOH)_2]$ **1** with $[Ni(cod)_2]$ (cod = cycloocta-1,5-diene) in the presence of extra triethylphosphine formed $[Mo_3Ni_2(\mu_4\text{-}S)(\mu_3\text{-}S)_3(\mu_3\text{-}Cl)(\mu_2\text{-}Cl)\text{-}Cl_2(PEt_3)_5]$ **13**.[70] The condensation is facilitated by the coordination of μ_2-S ligands to zero-valent nickel atoms and formation of new Mo–Ni bonds by displacement of two methanol ligands on the molybdenum atoms. The structure (Fig. 13) shows that the mixed-metal cluster core is Mo_3Ni_2 square pyramid in which one of the μ_2-S in **1** has been changed into μ_4-S and one of the terminal Cl atoms into a μ_2-Cl ligand bridging two molybdenum atoms and the other into μ_3-Cl capping the $MoNi_2$ triangle. The similar reaction of **1** with $[Pt(cod)_2]$ gave $[Mo_3Pt_2(\mu_3\text{-}S)_3(\mu_2\text{-}S)Cl_4(PEt_3)_6]$ **14**.[71] The cluster core (Fig. 14) of **14** is different from that of **13** and is a flat raft-type with two platinum atoms bridging the Mo–Mo edges. Two triethylphosphine ligands are coordinated to each platinum atom and chlorine ligands are all terminal. Two of the μ_2-S ligands in **1** are converted into μ_3-S ligands capping the Mo_2Pt triangles.

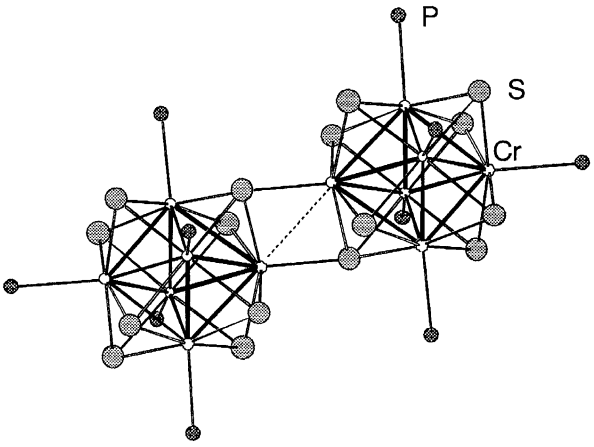

Fig. 12. Structure of $[Cr_{12}S_{16}(PEt_3)_{10}]$ **12**.

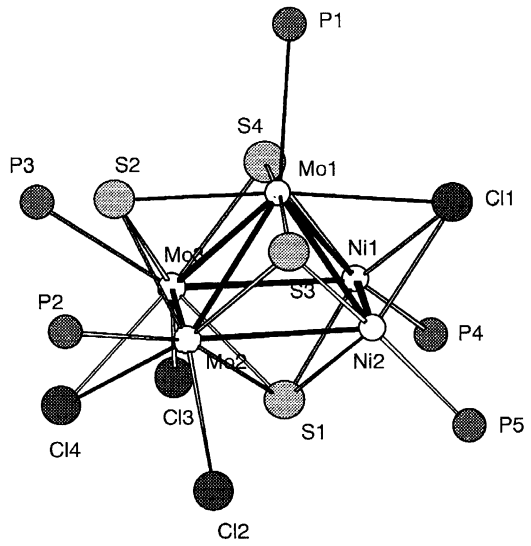

Fig. 13. Structure of $[Mo_3Ni_2S_4Cl_4(PEt_3)_5]$ **13**.

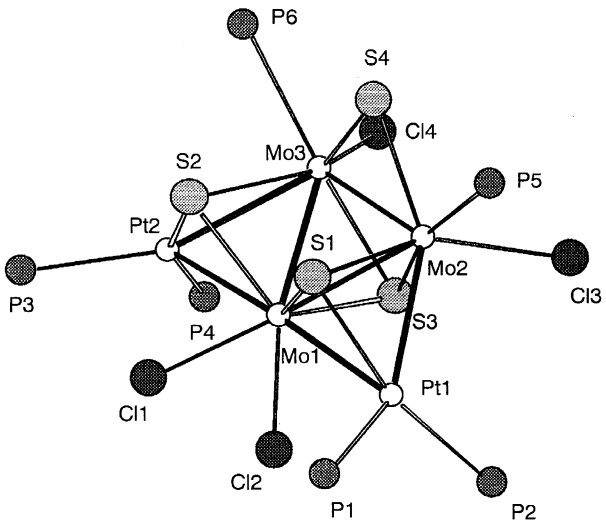

Fig. 14. Structure of $[Mo_3Pt_2S_4Cl_4(PEt_3)_6]$ **14**.

Distortion of Octahedral Clusters

The relationship between the cluster shape and cluster valence electrons is one of the central problems in the theoretical cluster chemistry.[72] The number of cluster valence electrons determines the number of the M–M bonding and the shape of a metal cluster framework. When HOMO is degenerate and partially filled with electrons, Jahn–Teller type distortion can be induced while keeping the global cluster shape.

In the distortion problem of the octahedral molybdenum cluster cores in the Chevrel phase compounds $M_xMo_6E_8$ (E = S, Se, Te), a theory emphasizing the electronic effects[73] has been modified by one stressing the steric effects.[74] The Chevrel phases are the solid state compounds in which the octahedral molybdenum cluster units are linked three-dimensionally. The extraction of pure electronic effects on the shape of the cluster units is difficult because the steric effects based on the intercluster bridges are often structure-determining. Isolation of the 20-electron molecular cluster complexes and their X-ray structures have shown that the molybdenum octahedra are very regular, in contrast with the most distorted cluster frameworks in the 20-electron solid state Chevrel phase compounds.[51,53] Therefore it is unlikely that the distortions in the solid state Chevrel phases with 20 electrons are caused mainly by electronic effects. However, the X-ray crystallography of a molecular crystal determines the structure of the molecules that is influenced by the crystal packing, and the structure does not always show the completely free molecules in vacuum. If we can estimate the crystal packing effects, we can know the structure of the isolated cluster skeleton.

This has become possible by the structural studies of the chromium cluster complexes $[Cr_6(\mu_3\text{-}E)_8(PR_3)_6]$. Since the six trialkylphosphine ligands are at the terminal positions of the Cr_6 octahedron, they form a P_6 octahedron around Cr_6. The cluster molecules contact with each other through the alkyl groups of the phosphine ligands and the crystal packing effects are reflected in the positions of the phosphorus atoms. The P–P and M–M (M = Cr, Mo) distances are listed in Table 2. It is apparent that the distortion of the Cr_6 octahedra parallels that of the P_6 octahedra, whereas the cores of the molybdenum cluster complexes show very little distortion. This difference has been attributed to the weaker metal–metal bonding in the chromium clusters.[60] In the case of triethylphosphine ligands, the P_6 octahedra for the chromium, molybdenum, and tungsten clusters are all regular indicating that the crystal packing effects are isotropic. Consequently, the cluster shapes can be handled as if they reflect the cluster cores of free molecules. If the M_6 cores distort, the origin of the distortion should be electronic. Since the M_6 cores in the 20-electron clusters of chromium, molybdenum, and tungsten with triethylphosphine ligands are all regular octahedra, the electronic effects to cause Jahn–Teller type distortion should be absent in these 20-electron cluster complexes. The distortion in the 20-electron Chevrel phase compounds is probably due to the intercluster linking.[24]

Electronic Structures and Spectral Assignments

Electronic-structure calculations are one of the bases for understanding the chemistry of the chalcogenide clusters. For example, all of the cluster chalcogenides of group 6 metals have strong colors. Absorption bands range from ultra-violet to visible regions and in many compounds near-infrared absorption bands also have been observed. We need electronic-structure calculations to understand these absorptions. However, the results of such calculations for the chalcogenide clusters are not very conclusive yet. Among chalcogenide clusters of group 6 metals, the electronic structures of the octahedral molybdenum clusters are most intensively studied.[75–81] The calculations have been conducted by various methods and their results show large differences in the degree of mixing of molybdenum and chalcogen orbitals. In the traditional view of the electronic structures of transition metal cluster complexes with π-donor ligands, the orbitals around the HOMO and the LUMO consist mainly of the metal d orbitals because the energies of metal orbitals are much higher than those of ligand orbitals (isolated metal-orbital model). The EH,[77,78] and LMTO-ASA calculations[63] give the results close to this model. On the other hand, the SW-Xα[75] and DV-Xα[81] methods show a large extent of mixing of metal and ligand orbitals (extensive-mixing model). Which picture is correct is still uncertain.

In the following, we discuss the electronic structures of chalcogen clusters calculated with the DV-Xα method.

Octahedral Clusters. We have calculated the electronic structures of $[Mo_6(\mu_3\text{-}E)_8(PH_3)_6]$ (E = S, Se) by using the DV-Xα (discrete-variational Xα) method and made the spectral (UV-vis and XPS) assignments of real compounds $[Mo_6(\mu_3\text{-}E)_8(PEt_3)_6]$ (Fig. 9)[51] based on both the calculated transition energies and oscillation strengths.[81] The calculated electronic spectra exhibit moderate agreements with the experimental spectra.(Fig. 15) The calculations show large mixing of the 4d(Mo) orbitals with 3p(S) and 4p(Se)orbitals. The relative energies of the valence orbitals near HOMO are mainly determined by the three types of interactions (1) Mo–L, (2) Mo–Mo, (3) L–L which are in the order (1) > (2) > (3), and not by the metal/ligand ratio of the constituting atomic orbitals.

The electronic structures of $[M_6(\mu_3\text{-}S)_8L_6]$ are strongly dependent on the metal M. The results of the DV-Xα calculations for $[M_6(\mu_3\text{-}S)_8(PH_3)_6]$ (M = Mo, Cr) and for $[Fe_6(\mu_3\text{-}S)_8(PH_3)_6]^{2+}$ are shown in Fig. 16. The calculations for the three clusters were performed under the same conditions except for geometry. The electronic structure of the iron cluster is very different from those of the chromium or molybdenum clusters and similar to the results of the previous calculations by Bencini et al.[82]

The electronic level diagrams for the molybdenum and chromium clusters in Fig. 16 show a gap above the LUMO (e_g) and the gap of the molybdenum cluster is larger than that of the chromium cluster. The MOs above the gap are metal–metal anti-bonding while those below the gap are metal–metal bonding or non-bonding. Therefore, the larger

Table 2. Interatomic Distances (Å) in the Octahedra of the Metal and Ligand

Compounds	M–M	Δ(M–M)	P–P	Δ(P–P)	Ref.
$[Cr_6S_8(PMe_3)_6]$	2.649—2.710	0.061	5.668—6.371	0.703	60
$[Cr_6S_8(PEt_3)_6]\cdot 2C_6H_6$	2.592—2.596	0.004	5.925—6.035	0.110	60
$[Cr_6Se_8(PMe_3)_6]$	2.723—2.787	0.064	5.784—6.435	0.651	60
$[Cr_6Se_8(PEt_3)_6]$	2.676—2.683	0.007	6.086—6.133	0.047	60
$[Cr_6Se_8(PMe_2Ph)_6]$	2.684—2.67	0.083	5.745—6.487	0.742	60
$[Cr_6Te_8(PEt_3)_6]$	2.896—2.953	0.057	6.258—6.456	0.198	61
$[Mo_6S_8(PMe_3)_6]$	2.635—2.637	0.002	5.875—6.470	0.595	52
$[Mo_6S_8(PEt_3)_6]$	2.662—2.664	0.002	6.179—6.291	0.112	51
$[Mo_6S_8(PMe_2Ph)_6]$	2.678—2.694	0.016	6.005—6.602	0.596	52
$[Mo_6Se_8(PEt_3)_6]$	2.701—2.708	0.007	6.190—6.402	0.218	51
$[W_6S_8(PEt_3)_6]$	2.678—2.681	0.003	6.174—6.310	0.136	32

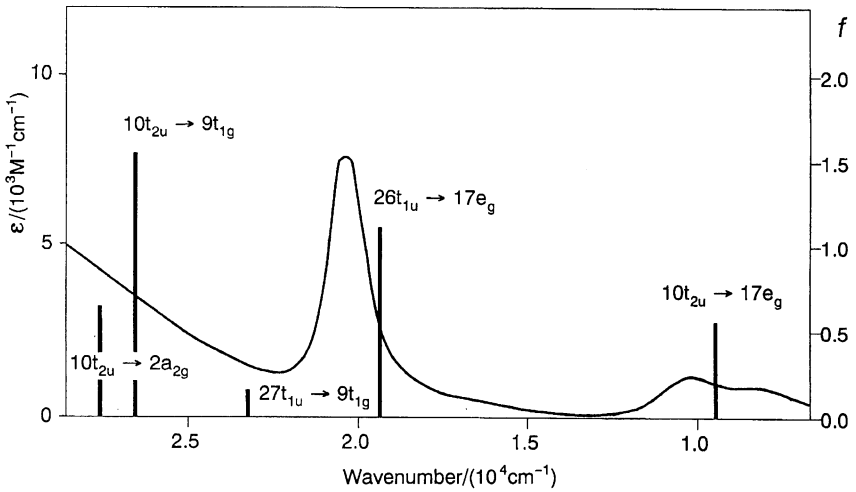

Fig. 15. Spectral assignments of $[Mo_6S_8(PEt_3)_6]$ based on the DV-Xα calculations of $[Mo_6S_8(PH_3)_6]$.

gap for the molybdenum cluster indicates the stronger interaction between metal atoms in the molybdenum cluster than in the chromium cluster. Stronger metal–metal bonds in the molybdenum cluster is supported by the discussion of the bond order n, which is calculated by the equation $\log n = (d_0 - d_1)/0.6$,[83] where d_1 is the observed metal–metal distance in $[M_6S_8(PEt_3)_6]$ (M = Mo, Cr)[51,60] and d_0 is the length for a single bond (d_0 = 2.619 Å for Mo and 2.383 Å for Cr). The calculated bond order n for the metal–metal bond in the molybdenum cluster is 0.84, which is much greater than the value 0.44 for the chromium cluster.

The calculated MOs for the molybdenum cluster show an extensive mixing of the molybdenum orbitals and sulfur 3p orbitals. The mixing is much weaker in the chromium cluster, and the calculated level diagram resembles the one expected for the isolated-metal-orbital model. These results suggest that the energies of the metal–metal bonding orbitals in the molybdenum cluster are closer to the sulfur 3p orbitals than those in the chromium cluster. The metal–metal bonding orbitals in the molybdenum cluster are more stabilized than those in the chromium cluster due to the stronger metal–metal interaction discussed above.

In the iron cluster, some of the metal–metal anti-bonding orbitals are occupied, and the metal–metal distances are large. The calculated level diagram for the iron cluster has no gap above the e_g level in contrast to the molybdenum and chromium clusters, which reflects the very weak metal-metal interaction. In the iron cluster, the metal–ligand interaction is the main factor that determines the electronic levels.

Tetranuclear Raft Clusters. Tetranuclear raft clusters $[Mo_4S_6X_2(PEt_3)_6]$ (X = SH, Cl, Br. Fig. 5) are electron-precise since they have ten metal cluster electrons and five metal–metal bonds. In these clusters, metal atoms are either octahedrally or trigonal-bipyramidally coordinated by the ligands. The metal d orbitals whose lobes are directed towards the ligands are used principally for the metal-ligand σ bondings, and other d orbitals can be used for the metal–metal bonding interactions. The d orbitals suitable for the metal–metal bonds are the t_{2g} orbitals (d_{xy}, d_{xz}, and d_{yz}) in the octahedral case and the e″ orbitals (d_{xz} and d_{yz}) in the trigonal-bipyramidal one. These orbitals interact also with sulfur orbitals through the π interaction. If the metal–metal bonds are full single bonds, the number of the bonds around a metal atom cannot exceed the number of the d orbitals available for metal–metal bonds. In the tetranuclear raft clusters, each of the two hinge molybdenum atoms has three d orbitals for the metal–metal bonding, and each of the two wing-tip atoms has two. Then, a tetranuclear raft cluster has ten AOs ($2\times(3+2)$) for the metal-metal bonds, and they make ten MOs. Five of the ten MOs will be bonding if these metal

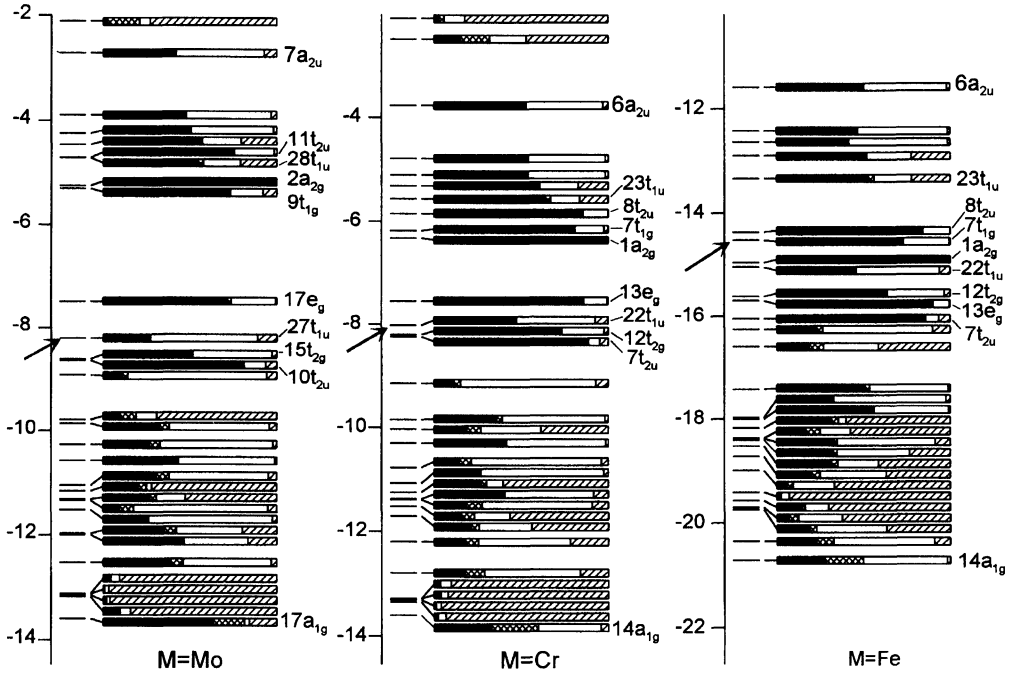

Fig. 16. Energy levels of MO for $[M_6S_8(PH_3)_6]$ (M = Mo and Cr) and $[Fe_6S_8(PH_3)_6]^{2+}$ calculated by spin-restricted DV-Xα method. Short horizontal lines just right of the vertical axis indicate the energies of the levels. The strips show the AO compositions of each MO: black, Mo-4d, Cr-3d, or Fe-3d; cross-hatched, Mo-5s, -5p, Cr-4s, -4p, or Fe-4s, -4p; white, S; hatched, PH_3. The arrow in each column shows the HOMO where the spin-paired configuration is assumed.

d orbitals are not strongly modified by the ligand orbitals through the metal-ligand π-interaction. The HOMO of the tetranuclear raft cluster with ten metal cluster electrons is the top of the five metal–metal bonding orbitals, and a gap is expected above the HOMO. The width of the gap is determined by the strength of the metal–metal interaction.

The electronic levels of the model compounds $[Mo_4S_6X_2(PH_3)_6]$ (X = SH, Cl, Br) with the C_{2h} symmetry have been calculated by using the DV-Xα method.[49] The HOMO-LUMO gaps in the calculations are the largest energy differences between the orbitals in the manifold of the valence levels (Fig. 17) and their values are considerably large (1.71 eV for SH, 1.52 eV for X = Cl, and 1.48 eV for X = Br). The DV-Xα calculation for the six-electron triangular cluster $[Mo_3S_4(H_2O)_6]^{4+}$ by Sakane et al. also gives a large HOMO-LUMO gap of 2.28 eV.[84] These results are consistent with the simple discussion described above. However, the calculated results in Fig. 17 show that the metal–metal bonding orbitals are strongly mixed with the ligand orbitals. While the two highest occupied orbitals ($64a_g$ and $38b_g$ for X = SH and Cl; $70a_g$ and $41b_g$ for X = Br) definitely have the nature of the metal–metal bonding, it is not very clear which orbitals in Fig. 17 correspond to the other three metal–metal bonding orbitals.

The large HOMO-LUMO gaps in the tetranuclear clusters indicate that the overall scheme of the MO levels is similar to those expected from the simpler picture described above in which the metal–ligand π-interaction is neglected. The results of the calculation show that the metal–metal bonding orbitals are not much destabilized by the metal–ligand π-interaction. This indicates that the metal–ligand π-interactions are not strong in these compounds. The metal–metal bonding orbitals and ligand orbitals are strongly mixed because their energies are close. Each metal–metal bonding orbital is distributed in several MOs of the same symmetry.

The above discussion for the tetranuclear raft clusters can be extended to other raft-type clusters. In the octahedral or trigonal-bipyramidal environment, the number of metal d orbitals available for the metal–metal bonds is three or two for each metal atom, and the number of the metal–metal bonds around the metal atom cannot exceed it if the metal–metal bonds are full single bonds. It is important to take the availability of the metal d orbitals for metal–metal bonds into account when we design new electron-precise clusters.

Trinuclear Clusters. The d orbitals of metal atoms make three a-type and three e-type orbitals in the trinuclear clusters.[18] An a-type orbital and an e-type orbital are bonding, and can accommodate six electron. In the next two molecular orbitals, which we will call intermediate orbitals, the interaction between metal orbitals are very weak due to their spatial arrangement, and the order of these two molecular orbitals are strongly influenced by the metal–ligand π interactions.

In the $M_3(\mu_3\text{-X})(\mu_2\text{-X})_3$ type clusters with the C_{3v} symmetry, the intermediate a_1 orbital is slightly Mo–Mo bonding, while the intermediate e orbital is weakly Mo–Mo antibonding. The metal–ligand π interactions strongly destabilize the a_1, and eight-electron clusters can be prepared only for bridging ligands with weak metal–ligand π interactions. In the seven-electron cluster complex $[Mo_3(\mu_3$-

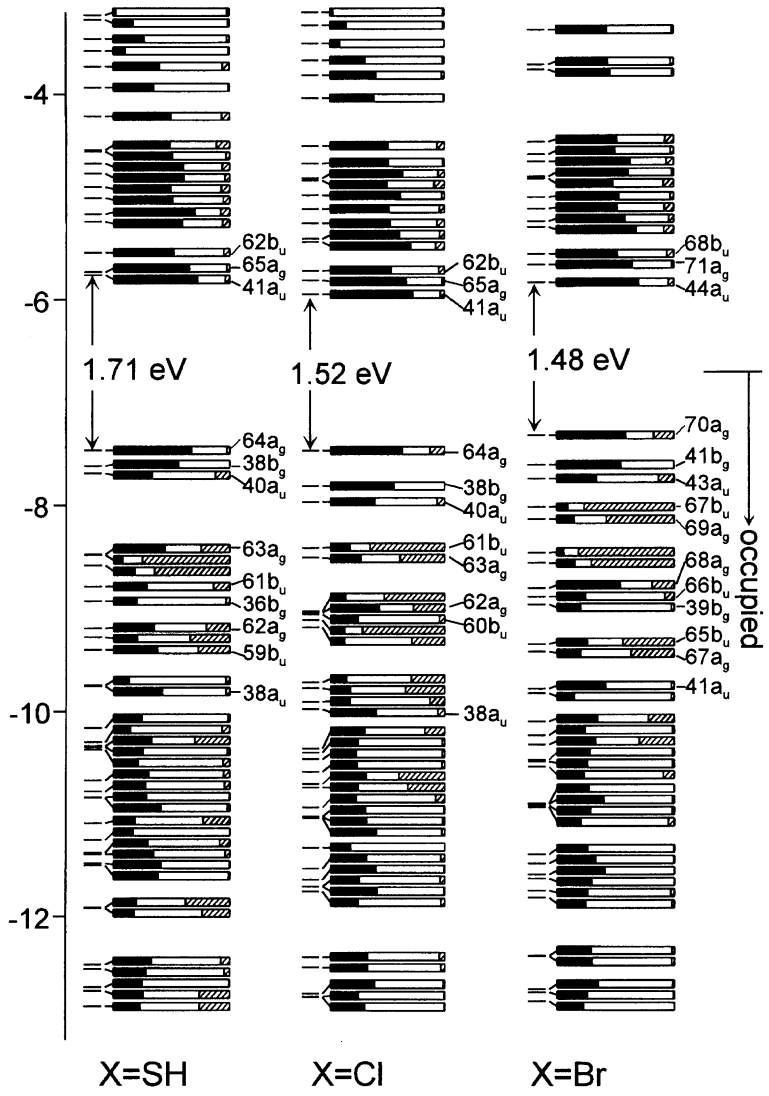

Fig. 17. Calculated energy levels for $[Mo_4S_6X_2(PH_3)_6]$ (X = SH, Cl, and Br). Short horizontal lines just right of the vertical axis indicate the energies of the levels. The strips show the AO compositions of each MO: black, Mo; white S and PH_3; hatched, X.

S)(μ_2-S)$_3$Cl$_3$(dppe)$_2$(PEt$_3$)] **4**, the Mo_3 core forms an almost equilateral triangle with the interatomic distances 2.804 and 2.809 Å, which are slightly longer than those in the six-electron $[Mo_3(\mu_3\text{-S})(\mu_2\text{-S})_3Cl_3(dmpe)_3]^+$ clusters (2.766 or 2.774 Å).[85,86] The equilateral geometry and elongation of the triangular core in **4** are not compatible with either of the electronic configuration. In a recent publication, Tatsumi et al. has suggested a subtle distortion in the seven-electron cluster compound $[(Cp^*Mo)_3(\mu_3\text{-S})(\mu_2\text{-S})_3]$ due to the Jahn–Teller effect by the occupation of the seventh electron in the e orbital.[45]

In triangular clusters with the $[Mo_3(\mu_3\text{-S})_2(\mu_2\text{-X})_3]$ core having the D_{3h} symmetry, the intermediate two orbitals are a_1'' and e″. When the cluster has eight electrons, two electrons must occupy one of these orbitals. Both a″ and e″ orbirals are antisymmetric in respect of the horizontal mirror plane, and only the e″ orbital can interact with the p orbitals of bridging sulfur atoms. If metal–ligand π interaction is not significant, weak metal–metal interaction will make the energy of the e″ oprbital lower and two electrons occupy the e″ orbital. This is the case for $[Mo_3(\mu_3\text{-S})_2(\mu_2\text{-Cl})_3Cl_6]^{3-}$ with the bridging chloro ligands, and the distortion to an isosceles triangle has been ascribed to Jahn–Teller effect by the energy surface calculations by the extended Hückel method.[87] However, if the bridging ligands are sulfur, the π interaction of lone-pair orbitals of bridging ligands with metal d orbitals is stronger and can reverse the level energies of the two orbitals. A sulfide cluster $[Mo_3(\mu_3\text{-S})_2(\mu_2\text{-S})_3(PMe_3)_6]$ has a perfect 3-fold symmetry in the crystal structure indicating no distortion.[34]

Isoelectronic Analogy

When a raft cluster M_{n+2} is composed of n metal triangles ($n \geq 1$) by fusion of edges and if each M–M bond requires two electrons to form a 2c–2e bond, the number of metal cluster electrons (MCE) is $4n+2$. (Such a raft cluster contains $N = n+2$ metal atoms and the MCE has been expressed as $4N-6$.[88]) (Fig. 18) On the other hand, the number of π-electrons in a polyacene with n fused benzene rings is also

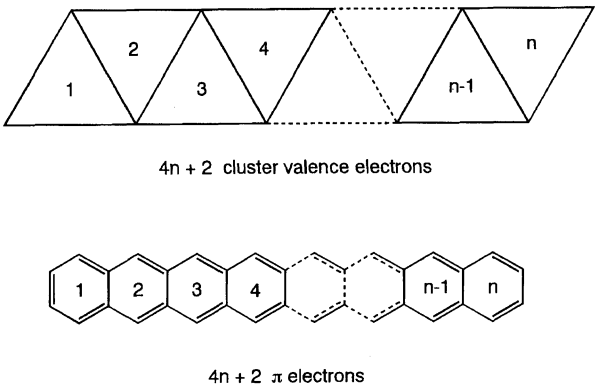

Fig. 18. Relationship between MCE in the raft cluster and π electrons in polyacene.

$4n+2$. Consequently, the number of MCE in a raft cluster with n triangular units and that of π-electrons in a polyacene with n fused benzene rings are equal. This **isoelectronic analogy** holds in any electron-precise raft cluster in either finite or infinite array of triangles if all the adjacent M–M are regarded as single-bonded, although combination of the metals with appropriate anionic ligands is necessary to attain the MCE suitable for the electron-preciseness (Table 3).

In the raft cluster system, lack of a M–M bond from an electron-precise cluster leads to reduction of MCE by 2. Correspondingly, in the polyacene system, addition of two hydrogen atoms leads to reduction of two π-electrons and hence the electron-deficient cluster compounds can be correlated to hydrogenated polyacenes as far as the number of electrons is concerned.

The above isoelectronic analogy can be applied to the real cluster compounds which have been isolated in our study and to the electrochemically (by CV) generated reduced or oxidized clusters.[89] Thus, Table 4 shows the correlation of the numbers of MCE in the cluster and the π-electrons in the hydrocarbons. The analogy between the $Mo_3(\mu_3\text{-}S)(\mu_2\text{-}S)_3$ type clusters and benzene has already been recognized by Lu and his coworkers[90,91] and has been expressed as quasi-aromaticity of the $[Mo_3S_4]^{4+}$ clusters. In a recent publication, Zhang refers to our hexanuclear cluster complex $[Mo_6(\mu_3\text{-}S)_4(\mu_2\text{-}S)_4(\mu_2\text{-}Cl)_2Cl_4(PEt_3)_6]$ as an equivalent of biphenylene $C_{12}H_8$.[92] Although the hexanuclear raft cluster (14-electron) looks like biphenylene structurally, the number of the π-electrons in biphenylene is only 12 and they are not isoelectronic. We prefer isoelectronic analogy because the raft type clusters with $Mo_{n+2}S_{2n+2}$ cores are composed of n interlacing incomplete cubanes Mo_3S_4, which is analogous to the fusion of benzene rings in polyacenes. Therefore we correlate the hexanuclear cluster (14-electron) to tetrahydrotetracene (14-electron).

Mixed Valence States of Cr_6S_8 and $Cr_{12}S_{16}$ Clusters

Cyclic Voltammetry. The chromium cluster complexes $[Cr_6(\mu_3\text{-}E)_8(PR_3)_6]$ are mixed-valence complexes comprising two Cr(II) and four Cr(III) metal centers. The cluster valence electrons are probably delocarized in the whole structure, and these cluster complexes are considered to belong to the class II or class III mixed-valence complexes according to the classical definition of Robin

Table 3. Isoelectronic Analogy between the Electron-Precise Sulfide Clusters and Aromatic Compounds

Number of core units n	Cluter compounds	Oxidation state of Mo	Number of MCE	Aromatic compound	Number of π-electrons
1	$[Mo_3S_4]^{4+}$	4	6	C_6H_6	6
2	$[Mo_4S_6]^{2+}$	3.5	10	$C_{10}H_8$	10
3	$[Mo_5S_8]$	3.2	14	$C_{14}H_{10}$	14
4	$[Mo_6S_{10}]^{2-}$	3	18	$C_{18}H_{12}$	18
n	$[Mo_{n+2}S_{2n+2}]^{6-2n}$	$(2n+10)/(n+2)$	$4n+2$	$C_{4n+2}H_{2n+4}$	$4n+2$

Table 4. Isoelectronic Analogy in the Real Compounds

n	Mo cluster core		Incomplete cubane	MCE or π-electrons	Hydrocarbon
1	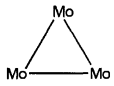	$[Mo_3S_4Cl_4(py)_5]$	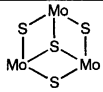	6	 C_6H_6
2	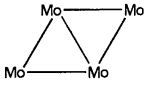	$[Mo_4S_6Cl_2(PMe_3)_6]$	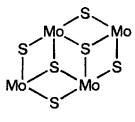	10	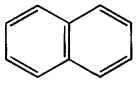 $C_{10}H_8$
4	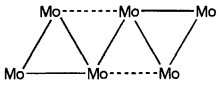	$[Mo_6S_8Cl_2(PEt_3)_6]$	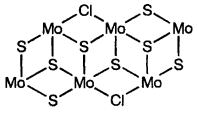	14	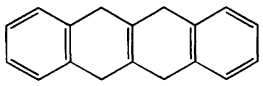 $C_{18}H_{16}$

and Day.[93] The cyclic voltammetry of $[Cr_6(\mu_3\text{-}S)_8(PEt_3)_6]$ in THF (Fig. 19) has shown an oxidation step at −0.86 V and a reduction step at −1.54 V versus Cp_2Fe^+/Cp_2Fe couple. The dimer cluster $[Cr_{12}(\mu_4\text{-}S)_2(\mu_3\text{-}S)_{14}(PEt_3)_{10}]$ has two oxidation steps at −0.86 and −0.44 V, and two reduction steps at −1.57 and −2.12 V versus Cp_2Fe^+/Cp_2Fe couple. (Fig. 20)[67,94] All the waves are assumed to be due to one-electron redox processes corresponding to one-electron redox of a Cr_6S_8 cluster unit. The electrochemistry suggests that there are $[Cr_6S_8\text{–}Cr_6S_8]$, $[Cr_6S_8^+\text{–}Cr_6S_8]$, $[Cr_6S_8^+\text{–}Cr_6S_8^+]$, $[Cr_6S_8^-\text{–}Cr_6S_8]$, and $[Cr_6S_8^-\text{–}Cr_6S_8^-]$ states. The potentials of the first redox process in $[Cr_6S_8\text{–}Cr_6S_8]$ are very near those of the $[Cr_6S_8]$ cluster and the electronic state in one of the Cr_6S_8 units in the Cr_{12} cluster should be very similar to the one of the Cr_6S_8 cluster complex. When one of the two cluster cores is either oxidized or reduced, the second redox step in the other cluster requires more oxidizing or more reducing potentials. It is very likely that a part of the electronic charge generated upon either oxidation or reduction is transmitted to the other cluster through the intercluster bonds. Alternatively the charged cluster unit should exert the electrostatic influence on the adjacent cluster. It was suggested that the extent of such electrostatic influence in the case of the mixed-valence $[Ru_3O(OAc)_6L_3]^{n+}$ dimer is much smaller than the effect due to electron delocalization.[95]

Magnetism. The hexanuclear chromium cluster complexes show temperature-dependent paramagnetism.[96] The χ_mT–T plots are shown in Fig. 21. Apparently the data do not conform to the Curie–Weiss law. $[Cr_6(\mu_3\text{-}S)_8(PEt_3)_6]$ formally contains four Cr(III) (d^3) and two Cr(II) (d^4) centers. As d^3 configuration has $S=3/2$ and d^4 either $S=2$ (high spin) or 1 (low spin), simple ferromagnetic addition and antiferromagnetic subtraction of the spins do not lead to the number of unpaired spins indicated from μ_{eff} values (1.7—2.5 μ_B).

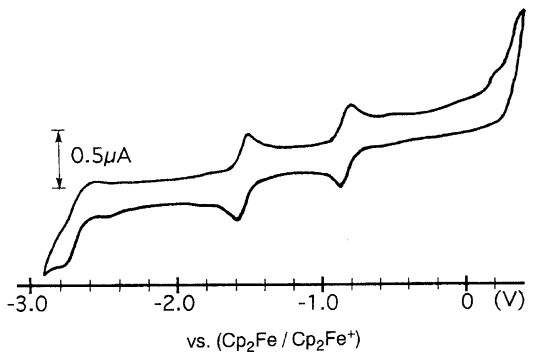

Fig. 19. Cyclic voltammogram of $[Cr_6S_8(PEt_3)_6]$ in THF.

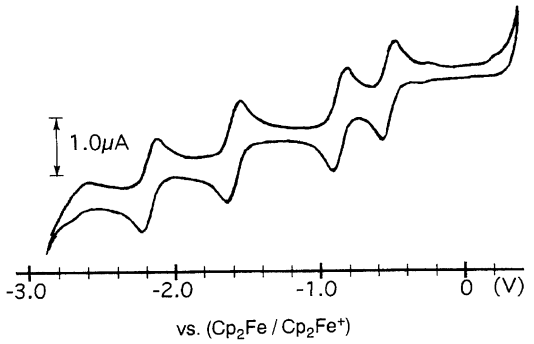

Fig. 20. Cyclic voltammogram of $[Cr_{12}S_{16}(PEt_3)_{10}]$ in THF.

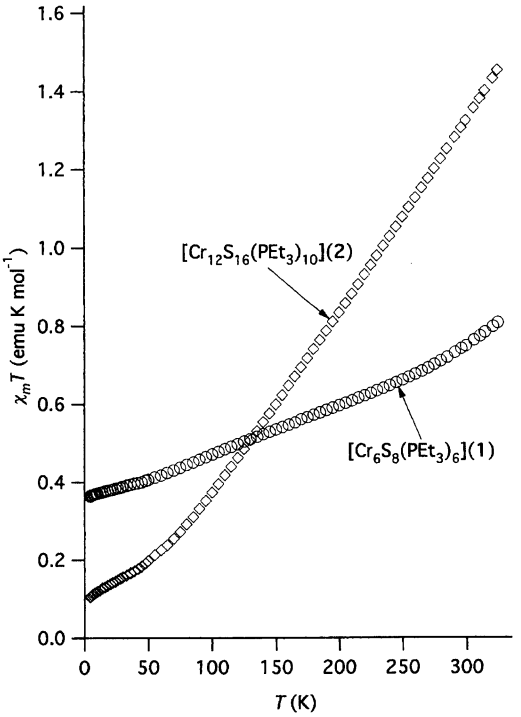

Fig. 21. The χ_mT–T curve for $[Cr_6S_8(PEt_3)_6]$ and $[Cr_{12}S_{16}(PEt_3)_{10}]$ between 4.5—330 K.

The DV-Xα MO calculations on $[Cr_6(\mu_3\text{-}S)_8(PH_3)_6]$ have shown that the cluster complex has a closed-shell configuration ($S=0$) for the structure with O_h symmetry and d(Cr–Cr) = 2.59 Å but the orbital energy levels are very sensitive to the Cr–Cr distance.[60] Slight elongation of the Cr–Cr distance (0.1 Å) changes the spin state into $S=2$. We postulate at present that the real cluster complexes also have spin states that increase from $S=0$ at ca.0 K to $S=2$ at higher temperatures, although the chromium clusters have been shown still paramagnetic at the lowest temperature (4.5 K) employed in our magnetic measurements.

It is interesting to note that the magnetic measurements on the tellurium derivative $[Cr_6(\mu_3\text{-}Te)_8(PEt_3)_6]$ in the temperature range 100—300 K has indicated Curie–Weiss behavior with two parallel spins and a triplet ground state has been assumed.[61] The paramagnetism has been ascribed to the weakness of the Cr–Cr interaction and smaller delocalization of spins as compared with that in the diamagnetic $[Mo_6(\mu_3\text{-}S)_8(PEt_3)_6]$.[51]

Magnetism of the relevant cluster complexes $[Fe_6(\mu_3\text{-}S)_8(PEt_3)_6]^{n+}$ ($n=1,2$) has been analyzed in detail by Bencini et al.[82,97] The complex $[Fe_6(\mu_3\text{-}S)_8(PEt_3)_6][PF_6]$ possesses a $S=7/2$ spin state well separated from the excited state and obeys Curie–Weiss law in the temperature range 4.2—300 K. The spin has been attributed to the ferromagnetic coupling of five low spin Fe(III) ($S=1/2$) and an intermediate spin Fe-

(II) ($S = 1$). The complexes $[Fe_6(\mu_3\text{-}S)_8(PEt_3)_6][PF_6]_2$[97] or $[Fe_6(\mu_3\text{-}S)_8(PEt_3)_6][BF_4]_2$[82] show a marked temperature dependence of the magnetic moments and their magnetic structures have been characterized empirically with the HDVV exchange spin Hamiltonian. Their χT–T curves look similar to those of the chromium cluster complexes and the magnetic interactions between the six metal atoms in the octahedral cluster cores may be also analogous although the calculated electronic structures of the chromium cluster and the iron cluster are very different (Fig. 16).[98,99]

The dodecanuclear cluster complex $[Cr_{12}(\mu_4\text{-}S)_2(\mu_3\text{-}S)_{14}(PEt_3)_{10}]$ has also temperature dependent paramagnetism, as shown in Fig. 21. The oxidation states of the chromium metals in the cluster complex are the same as those in the hexanuclear cluster complexes. The $\chi_m T$ values are about the double of those in $[Cr_6(\mu_3\text{-}S)_8(PEt_3)_6]$ at 330 K, reflecting the existence of two octahedral cluster units in the dodecanuclear cluster complex, but they decrease more rapidly to ca. 1/4 at 4.5 K. The data can be interpreted qualitatively in terms of the extra antiferromagnetic coupling, which is enhanced at lower temperatures, between the paramagnetic octahedral cluster units through Cr–S and Cr–Cr bonding interaction. The antiferromagnetic coupling between the paramagnetic $[Co_6(\mu_3\text{-}S)_8(PEt_3)_6]^+$ cluster complexes has been considered as the major driving force to form the diamagnetic dimer $[Co_{12}(\mu_4\text{-}S)_2(\mu_3\text{-}S)_{14}(PEt_3)_{10}]^{2+}$ which has similar cluster connectivity.[68,100] In this dodecanuclear cluster, the intercluster Co–Co distance is as short as 2.64 Å and the shortness has been attributed to the strong interaction between the unpaired spins localized on the coupling cobalt atoms in the $[Co_6(\mu_3\text{-}S)_8(PEt_3)_5]^+$ with one triethylphosphine missing. The relatively long intercluster Mo–Mo distance (3.40 Å) in the $[Mo_{12}(\mu_4\text{-}S)_2(\mu_3\text{-}S)_{14}(PEt_3)_{10}]$[69] formed from two diamagnetic $[Mo_6(\mu_3\text{-}S)_8(PEt_3)_6]$ may be an indication that spin-pairing between the paramagnetic octahedral clusters has a pronounced influence upon the shortening of the intercluster M–M distance.

We wish to acknowledge the contributions of the students of Osaka University and the University of Tokyo referred to in our papers. The work has been supported by the Grant-in-Aid for Scientific Research (Nos. 63430010, 02453037, 03640512, 06403009) and Grant-in-Aid for Scientific Research on Priority Area (No. 04241102) from the Ministry of Education, Science, Sports and Culture.

References

1) M. H. Chisholm, "Early Transition Metal Cluster with π-Donor Ligands," VCH, New York (1995).
2) T. Saito, in "Early Transition Metal Cluster with π-Donor Ligands," ed by M.H. Chisholm, VCH, New York (1995), pp, 63—164.
3) I. Dance and K. Fisher, *Prog. Inorg. Chem.*, **41**, 637 (1994).
4) M. G. Kanatzidis and S. P. Huang, *Coord. Chem. Rev.*, **130**, 509 (1994).
5) L. C. Roof and J. W. Kolis, *Chem. Rev.*, **93**, 1037 (1993).
6) T. Shibahara, *Coord. Chem. Rev.*, **123**, 73 (1993).
7) R. H. Holm, *Adv. Inorg. Chem.*, **38**, 1 (1992).
8) T. Shibahara, *Adv. Inorg. Chem.*, **37**, 143 (1991).
9) D. Coucouvanis, *Acc. Chem. Res.*, **24**, 1 (1991).
10) O. Pena and M. Sergent, *Prog. Solid State Chem.*, **19**, 165 (1989).
11) D. Fenske, J. Ohmer, J. Hachgenei, and K. Merzweiler, *Angew. Chem., Int. Ed. Engl.*, **27**, 1277 (1988).
12) P. Zanello, *Coord. Chem. Rev.*, **83**, 199 (1988).
13) A. Perrin, C. Perrin, and M. Sergent, *J. Less-Common Met.*, **137**, 241 (1988).
14) R. Chevrel, M. Hirrien, and M. Sergent, *Polyhedron*, **5**, 87 (1986).
15) A. Müller, *Polyhedron*, **5**, 323 (1986).
16) V. E. Fedorov, A. V. Mishchenko, and V. P. Fedin, *Russ. Chem. Rev.*, **54**, 408 (1985).
17) J. D. Corbett, *J. Solid. State. Chem.*, **37**, 335 (1981).
18) A. Müller, R. Jostes, and F. A. Cotton, *Angew. Chem., Int. Ed. Engl.*, **19**, 875 (1980).
19) W. Cen, F. M. MacDonnell, M. J. Scott, and R. H. Holm, *Inorg. Chem.*, **33**, 5809 (1994).
20) K. D. Demadis and D. Coucouvanis, *Inorg. Chem.*, **34**, 436 (1995).
21) T. Saito, N. Yamamoto, T. Yamagata, and H. Imoto, *J. Am. Chem. Soc.*, **110**, 1646 (1988).
22) T. Saito, M. Nishida, T. Yamagata, Y. Yamagata, and Y. Yamaguchi, *Inorg. Chem.*, **25**, 1111 (1986).
23) T. Saito, H. Manabe, T. Yamagata, and H. Imoto, *Inorg. Chem.*, **26**, 1362 (1987).
24) T. Saito, *Adv. Inorg. Chem.*, **44**, 45 (1996).
25) S. C. Lee and R. H. Holm, *Angew. Chem., Int. Ed. Engl.*, **29**, 840 (1990).
26) J. R. Long, A. S. Williamson, and R. H. Holm, *Angew. Chem., Int. Ed. Engl.*, **34**, 226 (1995).
27) A. A. Opalovskii, V. E. Fedorov, and K. A. Khaldoyanidi, *Dokl. Akad. Nauk SSSR*, **182**, 1095 (1968).
28) J. Marcoll, A. Rabenau, D. Mootz, and H. Wunderlich, *Rev. Chim. Miner.*, **11**, 607 (1974).
29) T. Saito, N. Yamamoto, T. Yamagata, and H. Imoto, *Chem. Lett.*, **1987**, 2025.
30) V. P. Fedin, S. P. Gubin, A. V. Mishchenko, and V. E. Fedorov, *Koord. Khim.*, **10**, 901 (1984).
31) F. A. Cotton, P. A. Kibala, and C. S. Miertschin, *Inorg. Chem.*, **30**, 548 (1991).
32) T. Saito, A. Yoshikawa, T. Yamagata, H. Imoto, and K. Unoura, *Inorg. Chem.*, **28**, 3588 (1989).
33) J. Mizutani, H. Imoto, and T. Saito, *Chem. Lett.*, **1994**, 2117.
34) K. Tsuge, H. Imoto, and T. Saito, *Inorg. Chem.*, **34**, 3404 (1995).
35) N. N. Timoshchenko, V. L. Kolosnichenko, S. V. Volkov, Y. L. Slovokhotov, and Y. T. Struchkov, *Koord. Khim.*, **16**, 1062 (1990).
36) S. Yamada, H. Imoto, and T. Saito, unpublished results.
37) T. Ando, Master's thesis, The University of Tokyo (1996).
38) J. Mizutani, H. Imoto, and T. Saito, *J. Cluster Sci.*, **6**, 523 (1995).
39) T. Shibahara and H. Kuroya, *Polyhedron*, **5**, 357 (1986).
40) T. Shibahara, M. Yamasaki, G. Sakane, K. Minami, T. Yabuki, and A. Ichimura, *Inorg. Chem.*, **31**, 640 (1992).
41) T. Shibahara, M. Yamasaki, T. Watase, and A. Ichimura, *Inorg. Chem.*, **33**, 292 (1994).
42) F. A. Cotton and R. Llusar, *Polyhedron*, **6**, 1741 (1987).
43) W. Beck, W. Danzer, and G. Thiel, *Angew. Chem., Int. Ed.*

Engl., **12**, 582 (1973).
44) H. Brunner, H. Kauermann, and J. Wachter, *J. Organomet. Chem.*, **265**, 189 (1984).
45) R. E. Cramer, K. Yamada, H. Kawaguchi, and K. Tatsumi, *Inorg. Chem.*, **35**, 1743 (1996).
46) K. Tsuge, H. Imoto, and T. Saito, *Inorg. Chem.*, **31**, 4715 (1992).
47) S. Kuwata, Y. Mizobe, and M. Hidai, *J. Chem. Soc., Chem. Common.*, **1995**, 1057.
48) S. Kobayashi, M. Sasaki, G. Sakane, and T. Shibahara, "The 45th Symposium on Coordination Chemistry of Japan," Fukuoka, 1995, Abstr., 1AP32.
49) K. Tsuge, S. Mita, Y. Fujita, H. Imoto, and T. Saito, *J. Cluster Sci.*, **7**, 407 (1996).
50) J. Mizutani, S. Yamada, H. Imoto, and T. Saito, *Inorg. Chem.*, **35**, 244 (1996).
51) T. Saito, N. Yamamoto, T. Nagase, T. Tsuboi, K. Kobayashi, T. Yamagata, H. Imoto, and K. Unoura, *Inorg. Chem.*, **29**, 764 (1990).
52) J. Sasahara, Master's thesis, The University of Tokyo (1992).
53) S. J. Hilsenbeck, V. G. Young, Jr., and R. E. McCarley, *Inorg. Chem.*, **33**, 1822 (1994).
54) X. Zhang and R. E. McCarley, *Inorg. Chem.*, **34**, 2678 (1995).
55) X. Xie and R. E. McCarley, *Inorg. Chem.*, **34**, 6124 (1995).
56) G. M. Ehrlich, C. J. Warren, D. A. Vennos, D. M. Ho, R. C. Haushalter, and F. J. DiSalvo, *Inorg. Chem.*, **34**, 4454 (1995).
57) F. Cecconi, C. A. Ghilardi, and S. Midollini, *Inorg. Chem. Acta*, **64**, L47 (1981).
58) F. Cecconi, C. A. Ghilardi, and S. Midollini, *J. Chem. Soc., Chem. Commun.*, **1981**, 640.
59) K. Tsuge, H. Imoto, and T. Saito, "The 43rd Symposium on Coordination Chemistry of Japan," Sendai, Japan, 1993, Abstr., 2A12.
60) K. Tsuge, H. Imoto, and T. Saito, *Bull. Chem. Soc. Jpn.*, **69**, 627 (1996).
61) B. Hessen, T. Siegrist, T. Palstra, S. M. Tanzler, and M. L. Steigerwald, *Inorg. Chem.*, **32**, 5165 (1993).
62) R. Chevrel and M. Sergent, in "Superconductivity in Ternary Compounds I," ed by Ø. Fischer and M. B. Maple, Springer, Berlin (1982), pp. 25—86.
63) H. Nohl, W. Klose, and O. K. Andersen, in "Superconductivity in Ternary Compounds I," ed by Ø. Fischer and M. B. Maple, Springer, Berlin (1982), pp. 165—221.
64) Ø. Fischer, *Appl. Phys.*, **16**, 1 (1978).
65) S. J. Hilsenbeck, R. E. McCarley, and A. I. Goldman, *Chem. Mater.*, **7**, 499 (1995).
66) R. E. McCarley, S. J. Hilsenbeck, and X. Xie, *J. Solid State Chem.*, **117**, 269 (1995).
67) S. Kamiguchi, H. Imoto, and T. Saito, *Chem. Lett.*, **1996**, 555.
68) F. Cecconi, C. A. Ghilardi, S. Midollini, and A. Orlandini, *Inorg. Chim. Acta*, **214**, 13 (1993).
69) S. Amari, H. Imoto, and T. Saito, unpublished results.
70) T. Saito, Y. Kajitani, T. Yamagata, and H. Imoto, *Inorg. Chem.*, **29**, 2951 (1990).
71) T. Saito, T. Tsuboi, Y. Kajitani, T. Yamagata, and H. Imoto, *Inorg. Chem.*, **30**, 3575 (1991).
72) D. M. P. Mingos and A. S. May, in "The Chemistry of Metal Cluster Complexes," ed by D. F. Shriver, H. D. Kaesz, and R. D. Adams, VCH, New York (1990), pp. 11—119.
73) K. Yvon, in "Current Topics in Material Science," ed by E. Kaldis, North-Holland, Amsterdam (1979), pp. 53—129.
74) J. D. Corbett, *J. Solid State Chem.*, **39**, 56 (1981).
75) L. Le Beuze, M. A. Makhyoun, R. Lissllour, and H. Chermette, *J. Chem. Phys.*, **76**, 6060 (1982).
76) J. K. Burdett and J. -H. Lin, *Inorg. Chem.*, **21**, 5 (1982).
77) T. Hughbanks and R. Hoffmann, *J. Am. Chem. Soc.*, **105**, 1150 (1983).
78) R. G. Wooley, *Inorg. Chem.*, **24**, 3519 (1985).
79) R. Arratia-Pérez, *Chem. Phys. Lett.*, **213**, 547 (1993).
80) C. Mealli, J. A. López, and Y. Sun, *Inorg. Chem. Acta*, **213**, 199 (1993).
81) H. Imoto, T. Saito, and H. Adachi, *Inorg. Chem.*, **34**, 2415 (1995).
82) A. Bencini, M. G. Uytterhoeven, and C. Zanchini, *Int. J. Quant. Chem.*, **52**, 903 (1994).
83) L. Pauling, "The Nature of the Chemical Bond," Cornell University Press, Ithaca, New York (1960), p. 400.
84) G. Sakane, T. Shibahara, and H. Adachi, *J. Cluster Sci.*, **6**, 503 (1995).
85) F. A. Cotton, R. Llusar, and C. T. Eagle, *J. Am. Chem. Soc.*, **111**, 4332 (1989).
86) F. A. Cotton, P. A. Kibala, M. Matusz, C. S. McCaleb, and R. B. W. Sandor, *Inorg. Chem.*, **28**, 2623 (1989).
87) Y. Jiang, A. Tang, R. Hoffmann, J. Huang, and J. Lu, *Organometallics*, **4**, 27 (1985).
88) F. A. Cotton and M. Shang, *J. Am. Chem. Soc.*, **110**, 7719 (1988).
89) J. Mizutani, H. Imoto, and T. Saito, unpublished results.
90) J. Q. Huang, J. L. Huang, M. Y. Shang, S. F. Lu, X. T. Lin, Y. H. Lin, M. D. Huang, H. H. Zhuang, and J. X. Lu, *Pure Appl. Chem.*, **60**, 1185 (1988).
91) Z. Chen, *J. Cluster Sci.*, **6**, 357 (1995).
92) Q. Zhang, *J. Cluster Sci.*, **6**, 357 (1995).
93) M. B. Robin and P. Day, *Adv. Inorg. Chem. Radiochem.*, **10**, 247 (1967).
94) T. Kamiguchi, H. Imoto, and T. Saito, "The 45th Conference on Coordination Chemistry," Japan, Fukuoka, 1995, Abstr., 1Aα11.
95) J. A. Baumann, D. J. Salmon, S. T. Wilson, and T. J. Meyer, *Inorg. Chem.*, **18**, 2472 (1979).
96) K. Tsuge, H. Imoto, and T. Saito, unpublished results.
97) A. Bencini, C. A. Ghilardi, S. Midollini, A. Orlandini, U. Russo, M. G. Uytterhoeven, and C. Zanchini, *J. Chem. Soc., Dalton Trans.*, **1995**, 963.
98) G. Blondin and J.-J. Girerd, *Chem. Rev.*, **90**, 1359 (1990).
99) A. Caneschi, D. Gatteschi, L. Pardi, and R. Sessoli, in "Perspectives in Coordination Chemistry," ed by A. F. Williams, C. Floriani, and A. F. Merbach, VCH, Weinheim, 1992, pp. 109—128.
100) C. Mealli and A. Orlandini, *Gazz. Chim. Ital.*, **125**, 271 (1995).

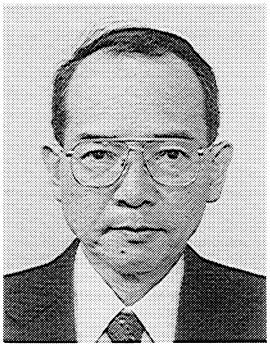

Taro Saito graduated from the University of Tokyo in 1961 and received a Doctor's degree from the University in 1966. He became Research Associate in Department of Industrial Chemistry in 1966 and spent postdoctoral years (1967—1969) at the laboratory of Professor M.L.H. Green of Oxford and moved to Department of Chemistry, Faculty of Science, the University of Tokyo in 1970. In 1982, he was appointed to Professor of Osaka University and spent seven years in Osaka. He returned to the University of Tokyo as Professor of Department of Chemistry in 1989. Saito contributed to the syntheses of transition metal alkyl, hydride, and dinitrogen complexes and since the days in Osaka his research efforts have been devoted to the field of transition metal cluster chemistry.

Hideo Imoto graduated from the University of Tokyo in 1972 and received a Doctor's degree from the University in 1977. He spent postdoctoral years at the laboratory of Professor J. D. Corbett in Ames (1977—1979) and at the laboratory of Professor A. Simon in Stuttgart (1979—1981). In 1984 he became Research Associate in Faculty of Engineering Science of Osaka University, moved to the University of Tokyo as a Lecturer in 1990, and became Associate Professor in 1995. He contributed to the syntheses, structural chemistry, and electronic-structure calculations of transition metal clusters and phosphates.